Available online at www.sciencedirect.com
ScienceDirect
Ceramics International 34 (2008) 359–364
CERAMICS INTERNATIONAL
www.elsevier.com/locate/ceramint

Microstructure and mechanical properties of hydroxyapatite obtained by gel-casting process

Biqin Chen, Tao Zhang, Jingxian Zhang, Qingling Lin, Dongliang Jiang *

The State Key Laboratory of High Performance Ceramics and Superfine Microstructure, Shanghai Institute of Ceramics, Chinese Academy of Sciences, Shanghai 200050, PR China

Received 16 June 2006; received in revised form 25 September 2006; accepted 21 October 2006
Available online 14 December 2006

Abstract

In the present work, well-shaped HAp green bodies were obtained by the gel-casting process with 50 vol.% slurry. After drying, the microstructure and pore distribution of the green body were investigated. The density, compressive strength and flexural strength of the green body were 1.621 g/cm^3, 32.6 ± 3.2 MPa and 13.8 ± 1.0 MPa, respectively. After pressureless sintering at the range of 1100–1300 °C for 2 h, the relative density of the final product ranges from 71.8 to 97.1% th. The maximum value of flexural strength, elastic modulus, hardness and fracture toughness were 84.6 ± 12.6 MPa, 138 ± 7 GPa, 4.45 ± 0.18 GPa and 0.95 ± 0.13 MPa m$^{1/2}$, respectively. SEM images show a compact and uniform microstructure; the average grain size was found by using the linear intercept method. XRD and FTIR determined the phase and the radical preserved after sintering.

Keywords: A. Suspensions; C. Mechanical properties; Microstructure

1. Introduction

Synthetic hydroxyapatite (HAp) has been used as a bone substitute because of its biocompatibility and chemical and biological affinity with bone tissues [1–2]. However, its clinical application has been limited due to the poor mechanical reliability [3]. Recently, a number of efforts have been made to improve the mechanical reliability of HAp ceramics obtained by a colloidal process [4–8]. Among these methods, gel-casting has significant advantages over the other processes, in terms of dimensional accuracy and complex shaping capabilities, the uniform structure and high strength of the green bodies. Therefore, the gel-casting method would be very useful to obtain pieces of HA with complex shapes, as is required for clinical applications.

Gel-casting, developed by Janney and co-workers [10–12], has rapidly developed in the past decade as a promising colloidal in situ forming technique. It has been applied in the forming of many sorts of ceramic material systems [14–17]. Moreover, it has been utilized in the forming of HAp porous ceramics [18–21]. In these works the solids loading of HAp slurry is usually very low, only about 50 wt.%. Padilla et al. [8,9] have prepared high solids loading (>50 vol.%) HAp slurries with low viscosity for preparation of compact HAp ceramics. But the HAp ceramics they got still had poor mechanical properties and phase impurity due to the high sintering temperature and long soaking time.

The aim of this work was to evaluate the mechanical properties of the pieces obtained by the gel-casting process and to study the influence of sintering temperature on the microstructure and the phase purity of HAp pieces. Pieces were obtained from slurries with 50 vol.% solids loading and low viscosity. The flexural strength, elastic modulus and hardness of HAp pieces sintered at different temperature were investigated. SEM images showed a compact and uniform microstructure; XRD and FTIR determined the phase and the radical preserved after sintering.

2. Experimental procedure

The HA powder was obtained by precipitation between calcium nitrate solution and diammonium hydrogen phosphate

* Corresponding author. Tel.: +86 21 5241 2606; fax: +86 21 5241 3122.
E-mail address: dljiang@sunm.shcnc.ac.cn (D. Jiang).

0272-8842/$34.00
doi:10.1016/j.ceramint.2006.10.021

solution at room temperature and pH 10. The initial powder was then treated at 900 °C for 2 h. Finally, the powder was wet-milled for 20 h to gain suitable particle size distribution and specific surface area. The as-obtained powder (d_{50} = 0.60 μm) was used as starting powder for this work. The phase composition of the as-dried HA powder and the calcined powder was analyzed by X-ray diffraction (XRD, Cu Kα, Rigaku, Japan). FTIR analyses were made on a Nicolet Nexus spectrometer.

The slurries were prepared by mechanical mixing, in a first stage, the dispersant, monomeric solution (monomer/binder = 13/1) and initiator was added to prepare a pre-solution. Then powder was progressively added to make 50 vol.% slurry within 1 h and agitated for a further 1 h. Rheological measurements were performed on a coaxial flat rheometry (SR-5 Rheomeric scientific instrument company, America). Measurements were performed in the shear rate range of 0.1–1000 s^{-1} at 20 °C. The viscosity data were recorded at constant shear rate 100 s^{-1}.

The as-obtained suspension was degassed in order to eliminate the air bubbles trapped inside the suspension before casting into moulds (50-mm length, 6-mm width and 7-mm height). Then the moulds were put in a water bath at 60 °C for 30 min in order to gel the system. The gelled pieces were carefully dried to avoid cracking. The density and pore distribution of green pieces was determined by Hg intrusion porosimetry in a Micromeritics ASAP2010 porosimeter. The compressive strength of the green bodies were measured using an Instron 5566 universal testing machine, at a crosshead speed of 2.5 mm/min. Three-point bending test was performed on the basis of Instron 5566 universal testing machine using specimens with dimensions of 3 mm in thickness, 4 mm in width and 36 mm in length at a crosshead speed of 0.5 mm/min. Five specimens were prepared for each strength test.

The green blocks were heated to 600 °C at a heating rate of 1.0 °C/min to burn out the monomers and other volatiles, followed by the pressureless sintering at different temperature (ranging from 1100 to 1300 °C) for 2 h.

The relative density and porosity of the sintered samples were determined by the Archimedes's method. The microstructure of the pieces was observed on the fractured surface and polished surface by scanning electron microscopy (SEM) (model EPMA-8705Q, HII, Shimadzu, Japan). The average grain size for different sintering temperature was found by using the linear intercept method. At least 50 grains were measured to get the average value. The flexural strength of HA ceramics was measured using an Instron 5566 universal testing machine by three-point bending, using a span of 30 mm and a crosshead speed of 0.5 mm/min. The indentation test was performed in a microhardness tester (IF, AkashIII, Japan), with a Vickers indenter, applying a load of 2.0 kg for 10 s. Interference lenses were used in the optic microscope to determine clearly the indentation. The fracture toughness (K_{IC}) of the samples was determined by using the indentation technique by measuring the crack length and using known equations [13]. At least five measurements were prepared for each test.

3. Results and discussions

3.1. Slurry preparation and characterization

Fig. 1a shows the viscosity of 40 vol.% Hap slurries versus concentration of dispersant. The dispersant used was Lopon890, a polyacrylic acid sodium salt (PAA-Na, BK Giulini, MW = 4000–5000). Initially, the viscosity decreases with increasing amount of dispersant and reaches the lowest point at 1.5 wt.% of dispersant.

Fig. 1b shows the viscosity curves of 50 vol.% slurry as a function of shear rate with 1.5 wt.% of dispersant. The slurry shows a shear-thinning behavior. The shear-thinning of HA slurry is a well-known characteristic of colloidally stable suspension at higher solids concentration [6]. In spite of high solids loading, the slurry only has a viscosity of 0.34 Pa s at the shear rate of 100 s^{-1}. This well-dispersed Hap slurries is required for gel-casting.

3.2. Characterization of green pieces

After casting, gelification and drying, well-shaped green bodies were obtained. Neither contraction nor cracking was observed. The pieces showed enough strength for demoulding and handling. The green samples' densities were 51.4% th. d. The value is lower than the common pressing pieces [23],

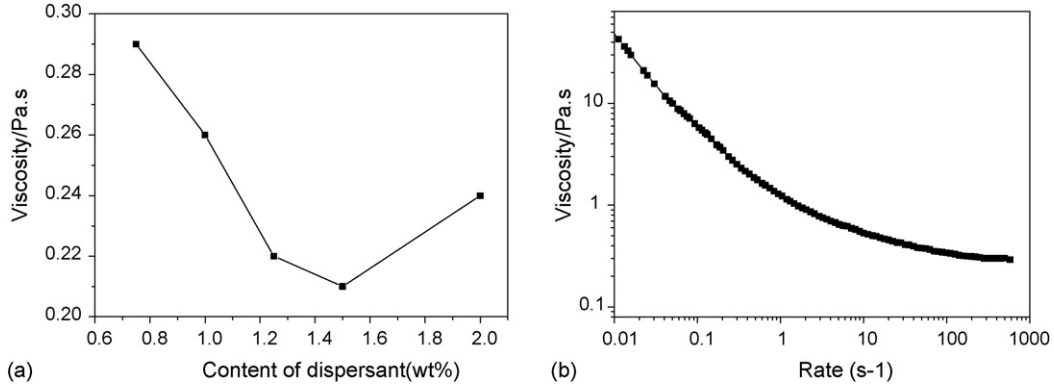

Fig. 1. (a) Influence of dispersant on the viscosity of slurries containing 40 vol.% HAp and (b) viscosity vs. shear rate for 50 vol.% HAp slurry.

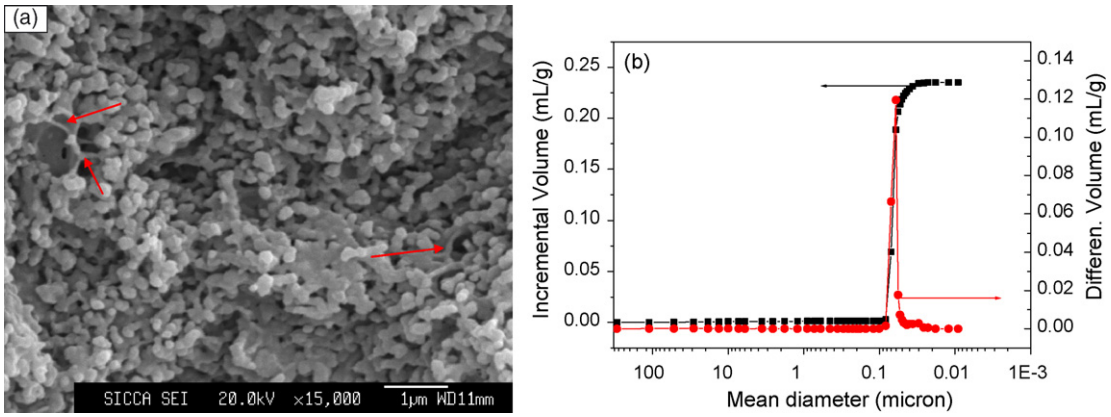

Fig. 2. The fracture SEM (a) and pore distribution (b) of 50 vol.% HAp green body.

similar as the other colloidal process [4,6]. On the contrary, the mechanical properties of green pieces are higher than other processes mentioned here. The green pieces have a compressive strength of 32.6 ± 3.2 MPa. The high strength comes from the cross-linking gel network and the homogenous packing of particles. This was confirmed in Fig. 2a. As shown by red arrows, the dried gel adhered to HAp particles and bound them together.

There are pores with different sizes in the green bodies. As shown in Fig. 2b, the pore diameter distribution, obtained by Hg intrusion porosimetry, showed a monomodal distribution type with the peak around 65 nm.

3.3. Characterization of sintered samples

The XRD patterns of the starting powder and HAp pieces sintered at different temperature are shown in Fig. 3. The HAp pieces after sintering were ground into powder. Compared with the card 9–432, there was no phase transformations detected when the sintering temperature was less than 1250 °C. However, when the sintering temperature was as high as 1300 °C, the X-ray analyses showed the presence of α-TCP phase, which indicates the decomposition of HAp. But the FTIR spectra still showed the bands of OH groups indicating that the active group of HA is preserved after sintering. As shown in the Fig. 4, the bands at 3570, 3460, 1610 and 633 cm^{-1} corresponding to OH group, together with the bands at 1090, 1040, 606 and 563 cm^{-1} are from PO_4^{3-} [22]. Also, the bands at 2930 cm^{-1} can be assigned to (P)O–H stretching vibration. With the increase in sintering temperature, some of the bands become weak. But as the sintering temperature of 1300 °C is reached, there are still bands corresponding to OH group, PO_4^{3-} and (P)O–H group. In a word, HAp had very limited phase decomposition between 1250 and 1300 °C, the main HAp phase and the active OH groups were preserved.

The density of sintered samples versus the sintering temperatures is shown in Fig. 5. The density increased with the increase in temperature and reached a maximum of 97.1 ± 0.2% at 1300 °C. The relative density of pieces sintered at 1100 °C was only 71.8 ± 0.4%. When the sintering temperature was higher than 1200 °C, the density versus sintering temperature curve was rather flat. The change of density is due to the different sintering process caused by the increasing sintering temperature.

Scanning electron micrographs of the polished and heat-etched surfaces of sintered bodies are shown in Fig. 6a–e. An increase in grain size is observed with an increase in the sintering temperature. It is observed that samples sintered at 1100 and 1150 °C contain many connective pores at the

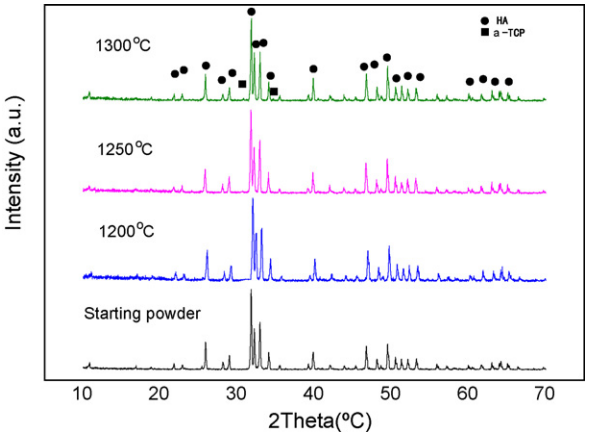

Fig. 3. XRD patterns of HA pieces sintered at different temperature.

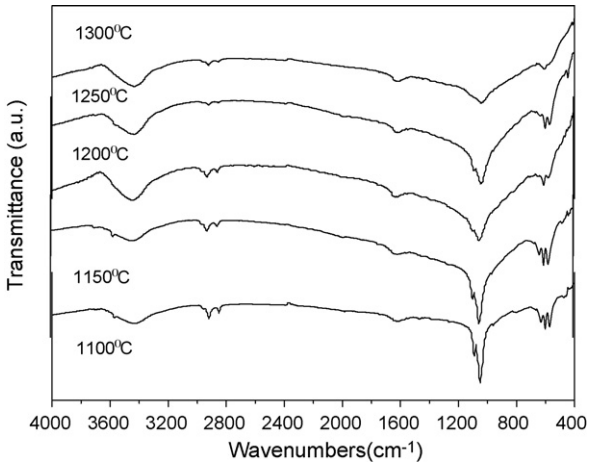

Fig. 4. FTIR spectra of HA pieces sintered at different temperature.

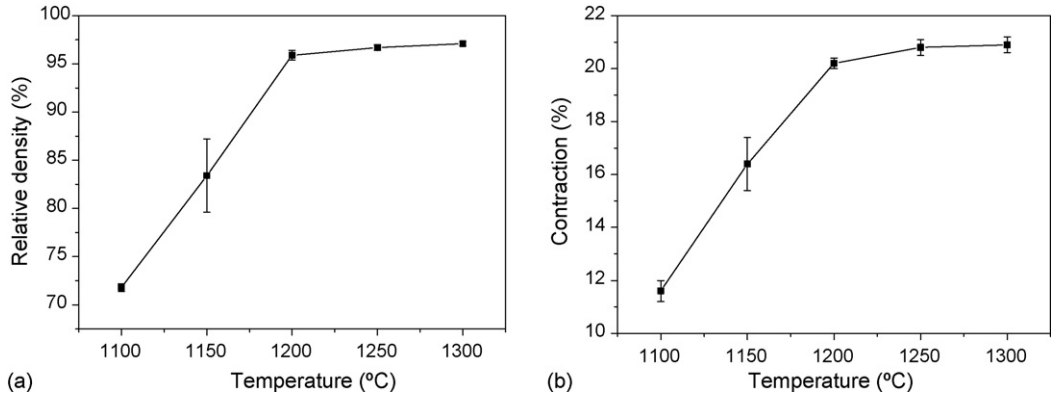

Fig. 5. Relative density (a) and contraction (b) of HAp pieces sintered at different temperature.

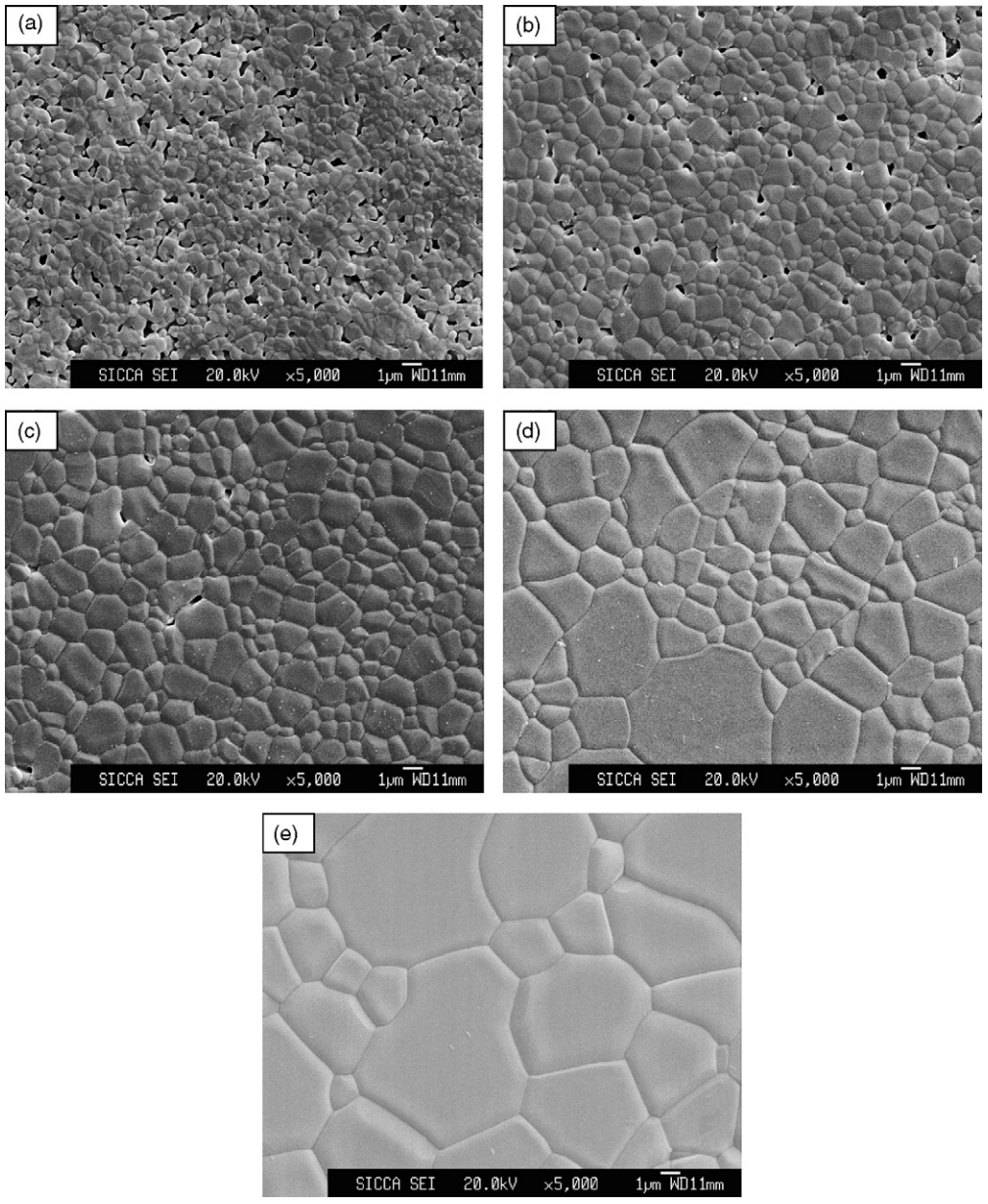

Fig. 6. SEM micrographs of polished surface of HAp pieces sintered at (a) 1100 °C, (b) 1150 °C, (c) 1200 °C, (d) 1250 °C and (e) 1300 °C for 2 h.

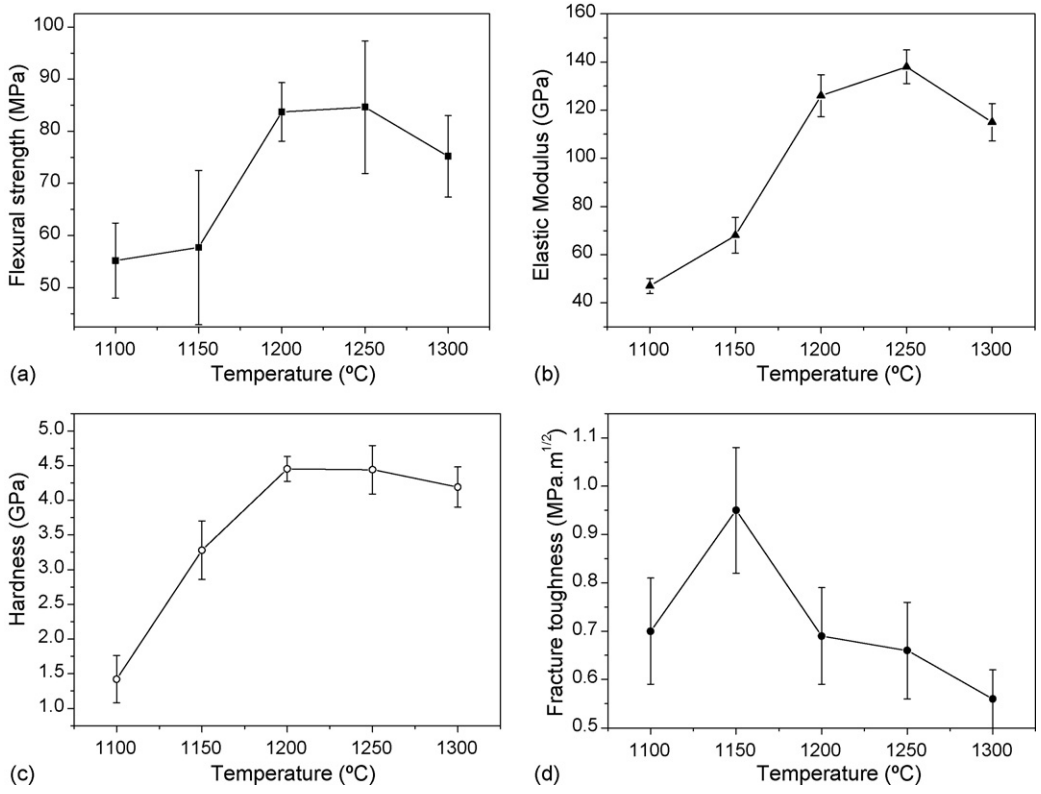

Fig. 7. Mechanical properties of HAp pieces sintered at different temperature: (a) flexural strength, (b) elastic modulus, (c) hardness and (d) fracture toughness.

Table 1
Average grain sizes (μm) of the HAp ceramics sintered at various temperatures

Sintering temperature (°C)	1100	1150	1200	1250	1300
Grain size (μm)	0.57 ± 0.15	0.83 ± 0.21	1.25 ± 0.31	2.13 ± 0.63	6.29 ± 2.73

boundaries and grain junctions, a few isolated pores are also found. At 1200 °C, the grains are fairly uniform and few isolated pores remain at the grain boundaries and grain junctions. At 1250 and 1300 °C, there is abnormal grain growth (>10 μm). Actually, there are more abnormal grains at 1300 °C than at 1250 °C. Table 1 shows the average grain size of the HAp ceramics sintered at various temperatures. At lower temperature (1100 °C), the grain size is about 0.57 ± 0.15 μm, similar to the size of the starting powder (d_{50} = 0.60 μm). The grain growth is enhanced with the increases in sintering temperature, at the same time the connective pores gradually disappear and the isolated pores form [24]. At the range of 1200–1250 °C, the densification process is almost complete; the grain size is 1.25 ± 0.31 and 2.13 ± 0.63 μm, respectively. At higher temperature (1300 °C), the compact process slows down but the average grain size increases significantly to 6.29 ± 2.73 μm with abnormal grain growth (>10 μm).

Fig. 7 shows the mechanical properties of HAp pieces sintered at different temperature. At least five measurements were prepared for each test. The pieces sintered at 1250 °C show maximum flexural strength value of 84.6 ± 12.6 MPa and maximum elastic modulus of 138 ± 7 GPa (Fig. 7a and b). However, at higher sintering temperatures the strength decreased. The microstructure of pieces sintered at 1300 °C show abnormal grain growth, which may be the reason for the strength decrement. The lower strength at lower temperature (1100–1200 °C) is caused by the low relative density and more pores in the samples. The flexural strength value is in the range of HAp ceramics reported, but the maximum elastic modulus is higher than reported [3]. Fig. 7c shows the dependence of hardness on sintering temperature. The maximum value of 4.45 ± 0.18 GPa appeared at 1200 °C, while the value at 1250 °C (4.44 ± 0.35) is nearly the same. The lower hardness of pieces sintered at 1100 and 1150 °C is caused by retarded densification [25]. In a brittle material like HAp, the fracture toughness is very low, as shown in Fig. 7d. The change in the fracture toughness with the sintering temperature is due to the combined influence of density and grain size. Decrease of K_{IC} with increasing grain size is usually observed in ceramics where the fracture mechanism is transgranular because the major contribution to crack resistance is related to the crossing of the grain boundaries [26].

4. Conclusions

The well-shaped HAp green bodies were obtained by gel-casting process with the solids loading of 50 vol.% slurry. After drying and binder burning, the pieces were heat treated in the

temperature range of 1100–1300 °C for 2 h. Compact HAp ceramics with homogenous microstructure and enhanced mechanical properties were obtained. The average grain size and relative density of pieces were in the range of 0.57–6.29 μm and 71.8–97.1%, respectively, due to the increasing sintering temperature. The maximum value of flexural strength, elastic modulus, hardness and fracture toughness were 84.6 ± 12.6 MPa, 138 ± 7 GPa, 4.45 ± 0.18 GPa and 0.95 ± 0.13 MPa $m^{1/2}$, respectively.

Acknowledgement

This work was supported by the Shanghai Science and Technology Committee (no. 06JC14071).

References

[1] L.L. Hench, Bioceramics: from concept to clinic, J. Am. Ceram. Soc. 74 (1991) 1487–1510.
[2] S.V. Dorozhkin, M. Epple, Biological and medical significance of calcium phosphate, Angew. Chem. Int. Ed. 41 (2002) 3130–3146.
[3] W. Suchanck, M. Yoshimura, Processing and properties of hydroxyapatite-based biomaterials for use as hard tissue replacement implants, J. Mater. Res. 13 (1998) 94–117.
[4] R. Rao, S.K. Kannan, Dispersion and slip-casting of hydroxyapatite, J. Am. Ceram. Soc. 84 (2001) 1710–1717.
[5] Z. Sadeghian, J.G. Heinrich, F. Moztarzadeh, Preparation of highly concentrated aqueous hydroxyapatite suspensions for slip casting, J. Mater. Sci. 40 (2005) 1–5.
[6] L.M. Rodríguez-Lorenzo, M. Vallet-Regí, J.M.F. Ferreira, Colloidal processing of hydroxyapatite, Biomaterials 22 (2001) 1847–1852.
[7] J.X. Zhang, M. Maeda, N. Kotobuki, M. Hirose, H. Ohgushi, D. L. Jiang, M. Iwasa, Aqueous processing of hydroxyapatite, Mater. Chem. Phys., in press.
[8] S. Padilla, R. García-Carrodeguas, M. Vallet-Regí, Hydroxyapatite suspensions as precursors of pieces obtained by gelcasting method, J. Eur. Ceram. Soc. 24 (2004) 2223.
[9] S. Padilla, M. Vallet-Regí, M.P. Ginebra, F.J. Gil, Processing and mechanical properties of hydroxyapatite pieces obtained by the gelcasting method, J. Eur. Ceram. Soc. 25 (2005) 375.
[10] M.A. Janney, Method for Forming Ceramic Powders into Complex Shapes. U.S. Patent 4,894,194 (1990).
[11] O.O. Omatete, M.A. Janney, R.A. Strehlow, Gelcasting—a new ceramic forming process, Am. Ceram. Soc. Bull. 70 (1991) 1641–1649.
[12] O.O. Omatete, M.A. Janney, R.A. Strehlow, Gelcasting: from laboratory development toward industrial production, J. Am. Ceram. Soc. 17 (1997) 407.
[13] K. Niihara, R. Morena, D.P.H. Hasselman, Evaluation of K_{1c} of brittle solids by the indentations method with low crack-to-indent ratios, J. Mater. Sci. Lett. 1 (1982) 13–16.
[14] A.C. Young, O.O. Omatete, M.A. Janney, P.A. Menchhofer, Gelcasting of alumina, J. Am. Ceram. Soc. 74 (1991) 612–618.
[15] O.O. Omatete, J.P. Pollinger, K. O'Young, Optimization of the gelcasting of a silicon nitride formulation, Ceram. Trans. 56 (1995) 337–343.
[16] Z.Z. Yi, Z.P. Xie, Y. Huang, J.T. Ma, Y.B. Cheng, Study on gelcasting and properties of recrystallized silicon carbide, Ceram. Int. 28 (2002) 369–376.
[17] O.O. Omatete, A. Blair, C.G. Westmoreland, A.C. Young, Gelcast zirconia–alumina composites, Ceram. Eng. Sci. Proc. 12 (1991) 2084–2094.
[18] H.R. Ramay, Miqin Zhang, Preparation of porous hydroxyapatite scaffolds by combination of the gel-casting and polymer sponge methods, Biomaterials 24 (2003) 3293–3302.
[19] P. Sepulveda, F.S. Ortega, Murilo D.M. Innocentini, V.C. Pandolfelli, Properties of highly porous hydroxyaptite obtained by the gelcasting of foams, J. Am. Ceram. Soc. 83 (2000) 3021–3024.
[20] L.M. Rodriguez-Lorenzo, M. Vallet-Regí, J.M.F. Ferreira, M.P. Ginebra, Hydroxyapatite ceramic bodies with tailored mechanical properties for different applications, J. Biomed. Mater. Res. 60 (2002) 159–166.
[21] P. Sepulveda, J.G.P. Binner, S.O. Rogero, O.Z. Higa, J.C. Bressiani, Production of porous hydroxyapatite by the gel-casting of foams and cytotoxic evaluation, J. Biomed. Mater. Res. 50 (2000) 27–34.
[22] N.K. Prashant, S. Charled, D.-H. Lee, D. Olton, D. Choi, Nanostructured calcium phosphate for biomedical applications: novel sythesis and characterization, Acta Biomater. 1 (2005) 65–83.
[23] N. Thangamani, K. Chinnakali, F.D. Gnanam, The effect of powder processing on densification, microstructure and mechanical properties of hydroxyapatite, Ceram. Int. 28 (2002) 355–362.
[24] R.J. Brook, Pore–grain boundary interactions and grain growth, J. Am. Ceram. Soc. 52 (1969) 339–340.
[25] R.W. Rice, C.C. Wu, F. Borchelt, Hardness–grain-size relations in ceramics, J. Am. Ceram. Soc. 77 (1994) 2539–2553.
[26] P. van Landuyt, F. Li, J.P. Keustermans, J.M. Streydio, F. Delannay, E. Muting, The influence of high sintering temperatures on the mechanical properties of hydroxyapatite, J. Mater. Sci.: Mater. Med. 6 (1995) 8–13.